Weaving Efficient Polymer Solar Cell Wires into Flexible Power Textiles

*Zhitao Zhang, Zhibin Yang, Zhongwei Wu, Guozhen Guan, Shaowu Pan, Ye Zhang, Houpu Li, Jue Deng, Baoquan Sun, and Huisheng Peng**

Due to the unique advantages of being lightweight and weaveable, photovoltaic devices in a flexible wire format have attracted increasing attentions in recent years.[1–3] Currently, these wire-shaped devices are mainly made by dye-sensitized solar cells. Liquid electrolytes were typically used similar to their conventional planar counterparts.[4–7] However, it is much more difficult to seal a long and flexible wire-shaped device, and the wire-shaped dye-sensitized solar cell is also not stable during the operation process. Recently, some attempts were made to explore wire-shaped polymer solar cells (PSCs) without liquid components.[8–10] The wire-shaped PSCs do not require sealing and can be directly used at a large scale.

The wire-shaped PSC had been generally made by twisting two fiber electrodes, and the interface between the fiber electrode and photoactive layer played a critical role on the photoelectric performance.[2] For instance, a low energy conversion efficiency of 0.15% was produced on the basis of perpendicularly aligned titania nanotube-modified Ti wire as a working electrode due to its less efficient contact with photoactive materials.[11] It is also critically important to develop high performance fiber electrodes as the conventional metal wires are sensitive to chemicals.[1] In addition, they are relatively rigid from a viewpoint of microdevices during the operation process. Therefore, although they were proposed to be organized into various electronic textiles by the well-developed weaving technology, to the best of our knowledge, it remains unavailable to realize them.

Here, a novel efficient wire-shaped PSC had been developed by incorporating a thin layer of titania nanoparticles between the photoactive material and electrode and introducing a flexible, strong, and conductive aligned carbon nanotube fiber electrode. The titania nanoparticle was found to enhance the adsorption of photoactive materials and charge transport, which had increased the energy conversion efficiency by 36% compared with the wire-shaped PSC without the titania nanoparticle under the same condition. The aligned carbon nanotube fiber enabled a high flexibility and stability for the resulting PSC. These miniature PSC wires had been further woven into flexible textiles that also exhibited high performances. For instance, as the resulting PSC textiles were lightweight and deformable, they were demonstrated to power portable electronic devices, a mainstream direction in the modern electronics.

Figure 1 schematically shows the structure of the wire-shaped PSC with a Ti wire and an aligned multiwalled carbon nanotube (MWCNT) fiber as cathode and anode, respectively. In a typical fabrication, a Ti wire was modified by growing aligned titania nanotubes on the surface by electrochemical anodization, followed by coating of a layer of titania nanoparticles. Two polymer layers of poly(3-hexylthiophene):phenyl-C_{61}-butyric acid methyl ester (P3HT:PCBM) and poly(3,4-ethylenedioxythiophene):poly(styrene sulfonate) (PEDOT:PSS) were then dip-coated onto the modified Ti wire. The resulting Ti wire was finally wound with an aligned MWCNT fiber to produce the wire-shaped PSC.

The lengths of titania nanotubes on the Ti wire were controlled by varying the growth time during the electrochemical anodization, e.g., 650 nm, 1.8 μm and 2.2 μm at 1, 10 and 15 min, respectively. The length of ≈1.8 μm that was shown to produce the highest energy conversion efficiency had been mainly studied in this work (Figure S1, Supporting Information). **Figure 2**a,b show top and side views of the aligned titania nanotubes with inner and outer diameters of 100 and 150 nm, respectively. Aligned titania nanotubes increased the charge separation and transport in the wire-shaped PSC. The resulting Ti wire was then treated with a $TiCl_4$ solution to produce

Z. Zhang, Z. Yang, G. Guan, S. Pan, Y. Zhang, H. Li, J. Deng, Prof. H. Peng
State Key Laboratory of Molecular Engineering of Polymers
Department of Macromolecular Science and Laboratory of Advanced Materials
Fudan University
Shanghai 200438, China
E-mail: penghs@fudan.edu.cn
Z. Wu, Prof. B. Sun
Institute of Functional Nano and Soft Materials
Soochow University
Suzhou, Jiangsu 215123, China

DOI: 10.1002/aenm.201301750

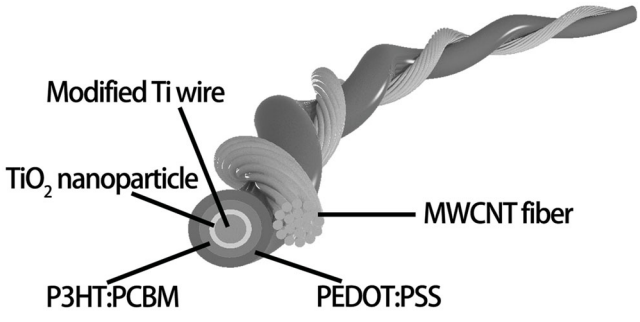

Figure 1. Schematic illustration to the wire-shaped PSC.

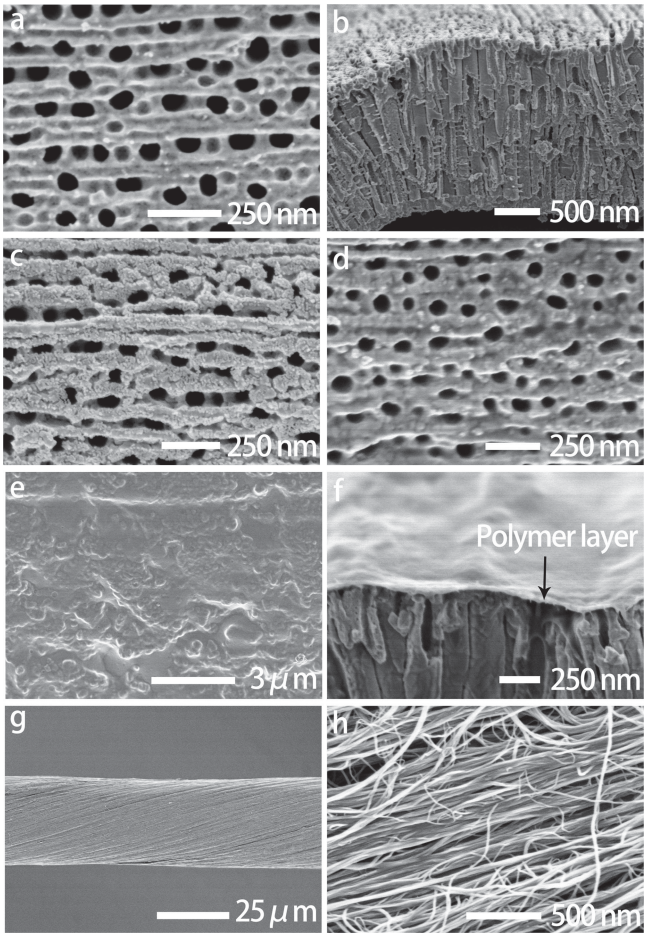

Figure 2. SEM images of two fiber electrodes. a,b) Aligned titania nanotubes by top and side views, respectively. c) Titania nanoparticle layer. d) P3HT:PCBM layer. e) PEDOT:PSS layer. f) P3HT:PCBM and PEDOT:PSS layers by a side view. g,h) MWCNT fiber at low and high magnifications, respectively.

titania nanoparticles on top surfaces of aligned titania nanotubes (Figure 2c). The use of titania nanoparticle increased the adsorption of photoactive materials and improved the charge transport.[12] The thicknesses of titania nanoparticles were easily controlled by varying the treatment time. **Figure 3** further shows typical scanning electron microscopy (SEM) images before and after treatments with the increasing time. The titania nanoparticles were firstly formed at the solid part and then also covered the hollow part of the titania nanotube array with the increasing time to 60 min. The sizes of nanoparticles were maintained to be almost the same of ≈20 nm until 30 min, and they agglomerated into larger aggregates (≈60 nm) with the further increase to 60 min.

The fabrication and structure characterization of the wire-shaped PSC had been made according to previous work.[13] A thin and continuous P3HT:PCBM layer was formed at the outer surface of the wire by dip coating (Figure 2d). Similarly, a thin and continuous PEDOT:PSS layer was also coated (Figure 2e) and used to improve the hole transport. The two

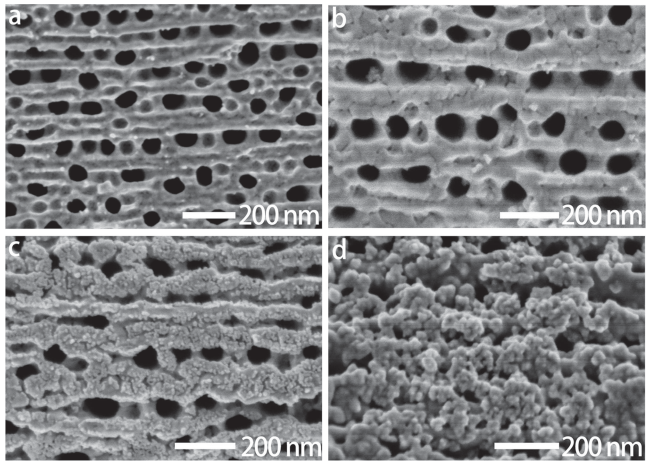

Figure 3. SEM images of titania nanotubes without and with $TiCl_4$ treatments under the increasing time. a) Without treatment. b) Treated by 15 min. c) Treated by 30 min. d) Treated by 60 min.

polymer layers were further verified to be uniform in thickness by a side view under SEM (Figure 2f). The thicknesses of the P3HT:PCBM and PEDOT:PSS layers were calculated to be appropriately 60 nm and 80 nm, respectively. Figure 2g,h show a typical MWCNT fiber with a diameter of ≈30 μm at low and high magnifications, respectively. The MWCNTs were highly aligned to enable both high mechanical strengths of $\approx 10^3$ MPa and electrical conductivities of $\approx 10^3$ S cm^{-1}.[14] The remarkable mechanical and electronic properties were important for the fabrication of wire-shaped PSCs.

Figure 4a–c show SEM images of a typical wire-shaped PSC at low and high magnifications. Although the wire-shaped PSC was flexible which will be discussed later, the Ti electrode seemed relatively rigid at local areas, so a highly flexible MWCNT fiber had been used as another electrode that can be tightly and closely twisted with the Ti wire. The pitch distance could be varied from hundreds of micrometers to millimeters that produced stable wire-shaped PSCs. Here the pitch distance of 750 μm was found to offer the highest efficiency and had been mainly investigated in this work. A lower pitch distance increased the covered MWCNT fiber electrode that shaded more incident lights with lower energy conversion efficiencies. In addition, the wire-shaped cell was less stable as the over-twisted two electrodes were separated from each other during use. A higher pitch distance decreased the contact area between two electrodes also with lower energy conversion efficiencies. In addition, the wire-shaped PSC became less stable as the two electrodes could not be tightly twisted.

The mechanism of the wire-shaped PSC is schematically shown in **Figure 5**a.[15] Upon the absorption of sunlight, the heterojunction layer generates excitons that are separated into electrons and holes. The holes are collected by the PEDOT:PSS layer and then transport to the aligned CNT fiber. The electrons are transported to the Ti wire through the titania layer. The layer of titania nanoparticles was critically important to produce efficient wire-shaped PSCs. Figure 5b shows current–voltage (*J*–*V*) curves of PSCs before and after being treated by

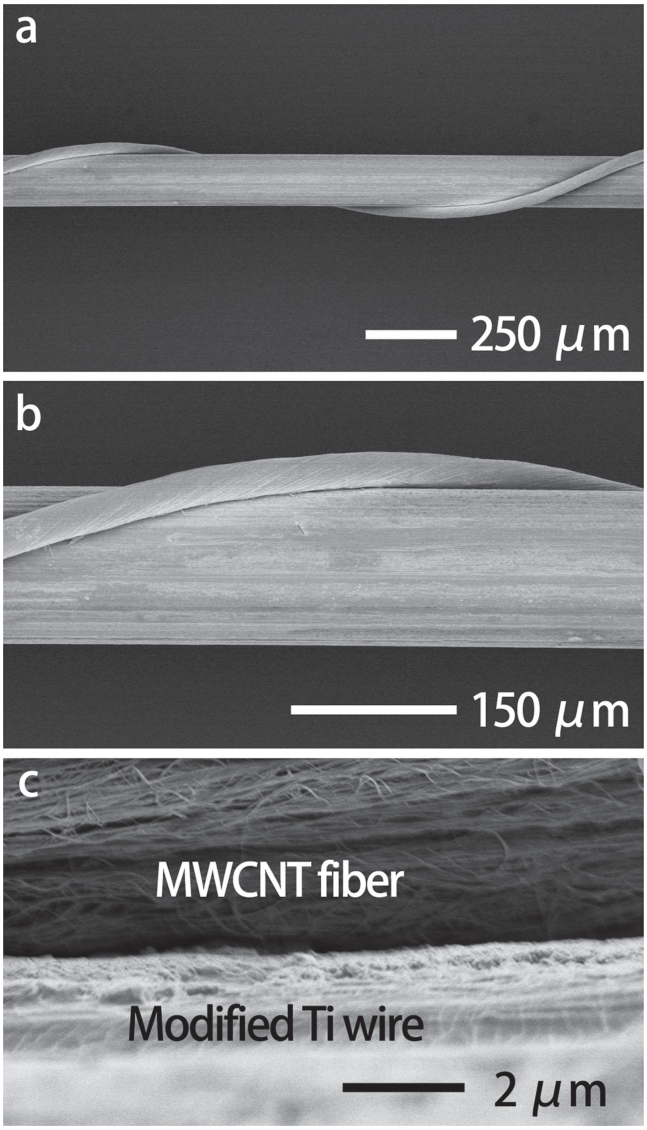

Figure 4. A wire-shaped PSC with increasing magnifications.

a $TiCl_4$ solution. The energy conversion efficiency (η) was calculated by the equation of $\eta = FFV_{oc}J_{sc}/P_{in}$, where FF, V_{oc}, J_{sc} and P_{in} represent fill factor, open-circuit voltage, short-circuit current density and incident light power density, respectively. The effective area was obtained by multiplying the length and diameter of the photoactive wire. The energy conversion efficiencies were lower than 1.31% without the treatment with an open-circuit voltage (V_{oc}) of 0.50 V, a short-circuit current density (J_{sc}) of 6.48 mA cm^{-2}, and a fill factor (FF) of 41%. The efficiencies were increased to 1.60% (V_{oc} of 0.53 V, J_{sc} of 7.38 mA cm^{-2}, and FF of 41%) and 1.78% (V_{oc} of 0.52 V, J_{sc} of 9.06 mA cm^{-2}, and FF of 38%) after treatments for 15 and 30 min, respectively. With the further increase in the treatment, the efficiency was decreased, e.g., 1.38% at 60 min (V_{oc} of 0.49 V, J_{sc} of 7.12 mA cm^{-2}, and FF of 40%) due to the agglomeration of titania nanoparticles into irregular and larger aggregates. Figure 5c shows incident photon-to-current efficiency (IPCE) curves of PSCs with and without treatments by $TiCl_4$. Obviously, the IPCE was increased with the increasing treated time to 30 min and then decreased with the further increase in the time, which agrees with the evolution of the energy conversion efficiency (Figure 5b).

The diameters of MWCNT fibers were also found to largely affect the wire-shaped PSCs (Figure 5d). The energy conversion efficiencies were increased from 0.72% to 1.78% with the increasing diameters from 18 to 32 μm and then decreased with the further increasing diameters (e.g., 1.47% and 1.18% at 60 and 74 μm, respectively). The maximal efficiency occurred at approximately 32 μm. A smaller fiber produced a higher electric resistance with a lower current density, while a bigger fiber shaded the incident sunlight also to decrease the current density.

The wire-shaped PSCs were flexible and could be easily deformed into various structures (**Figure 6**a). No obvious damages were found by SEM, and the energy conversion efficiencies had been maintained by ≈85% after bending for 1000 cycles (Figure 6b). These wire-shaped PSCs were also highly stable compared with the wire-shaped dye-sensitized solar cells. For instance, the energy conversion efficiencies had been maintained by over 70% without sealing in air after 16 days (Figure 6c).

A wide variety of microsized metal wires had been also studied to replace the MWCNT fiber but with much lower energy conversion efficiencies. For instance, Figure S2 (Supporting Information) shows a typical *J–V* curve from a wire-shaped PSC with an energy conversion efficiency of 0.48% based on a silver wire as the counter electrode to replace the MWCNT fiber. This difference can be explained by two facts. On the one hand, the MWCNT fiber with the working function of (4.8–5.1) eV is effective for the hole collection. In contrast, the metal wire such as silver with the work function of 4.3 eV is much less effective for the hole collection. On the other hand, the metal wires were not flexible enough for the wire-shaped PSCs with high efficiencies. For the silver wire, obvious gapes appeared between the modified Ti wire and silver wire (Figure S3a,b, Supporting Information). It became even worse under bending (Figure S3c,d, Supporting Information). As a result, in the case of the silver wire, the energy conversion efficiency was further severely decreased from 0.48% to 0.14% after bending by 50 cycles (Figure S4, Supporting Information).

The nanocrystalline semiconductor oxide layer played a crucial role in providing pathways for charge transport. For the nanoparticles that typically formed a network structure, the charges were easily trapped with long diffusion lengths and recombined at boundaries among particles with low efficiencies. In contrast, the charges have a far more direct route to the titanium electrode in aligned nanotubes compared to nanoparticle layers.[16–18] However, these aligned titania nanotubes showed much lower efficiencies than expected. The phenomenon may be explained by the following fact. The original Ti wire was smooth on the surface; after the growth of perpendicularly aligned nanotubes, the resulting outer surface became rugged. Therefore, it was difficult to produce thin

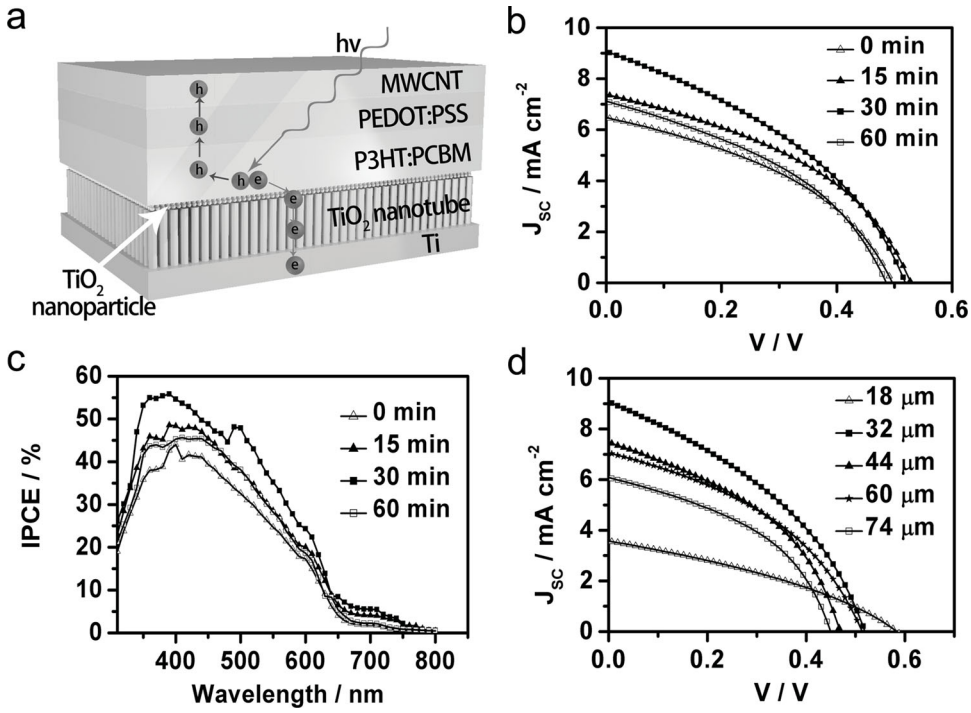

Figure 5. a) Schematic illustration of the mechanism. b) *J–V* curves without and with $TiCl_4$ treatments under the increasing growth time. c) IPCE curves without and with $TiCl_4$ treatments with increasing growth times. d) *J–V* curves for MWCNT fibers with increasing diameters.

and uniform P3HT:PCBM and PEDOT:PSS layers at the surface of the working electrode. Here the incorporation of semiconducting nanoparticles at the tips of aligned TiO_2 nanotubes after $TiCl_4$ treatment helped to make the outer surface uniform. In addition, the nanoparticle layer had effectively increased the polymer load, decreased the electrical resistance for charge transport and enhanced the light scattering.[17] Note that the outer polymer layer may slightly decrease the light access to the nanoparticle layer. Here this effect was not obvious as the ultra-thin polymer layers were transparent with high optical transmittances.[19]

The as-prepared wire-shaped PSC could be easily woven into various flexible structures such as textiles without the necessity for sealing that had been required by the widely studied wire-shaped dye-sensitized solar cells (Figure S5, Supporting Information, and Figure 7a,b). **Figure 7**c further shows the dependence of voltage on the number of wire-shaped PSCs that were woven and connected in series in the PSC textile. Obviously, the voltages are linearly increased with the increasing number of wire-shaped PSCs. Therefore, it is effective to scale up their applications by the well-developed weaving technology, e.g., various wearable electronic products. As expected, these PSC textiles were also highly flexible, and the energy conversion efficiencies had been maintained by ≈80% after bending for 1000 cycles (**Figure 8**a). Interestingly, these powering textiles could efficiently work independent on the incident angle, e.g., the energy conversion efficiencies were varied in less than 20% in the different angles (Figure 8b).

In conclusion, we have developed a family of novel wire-shaped PSCs with high performances by introducing a thin layer of titania nanoparticles that increased the charge separation and transport and an aligned MWCNT fiber anode that increased their stability. These miniature PSC wires could be directly used without sealing and easily scaled up by the well-developed textile technology.[20] The resulting flexible PSC clothes are described as lightweight and deformable power sources for portable electronic devices.

Experimental Section

The preparation of the electrode materials and fabrication of the wire-shaped PSCs were made according to the previous report.[13] MWCNT fibers were prepared by twisting aligned MWCNT sheets that had been drawn from a spinnable array with thickness of 220 μm. The spinnable array was synthesized by chemical vapor deposition.[21–23] Aligned titania nanotubes were grown on the Ti wire by electrochemical anodization.[24] The Ti wire (diameter of 127 μm) was firstly washed by acetone, isopropanol, and deionized water, respectively. Ethylene glycol solution in a solvent mixture of NH_4F (0.3%) and H_2O (8%) was used as the electrolyte. The growth was made by a two-electrode system with Ti wire and Pt plate as anode and cathode at 60 V for 10 min, respectively. The modified Ti wire was rinsed with deionized water and annealed at 500 °C for 1 h in air. The resulting Ti wire was immersed in 100 mM $TiCl_4$ solution at 70 °C for 30 min, washed by deionized water, and annealed at 450 °C for 30 min. The two polymer layers were dip-coated onto the modified Ti wire. The treated Ti wire was dipped into a chlorobenzene solution of P3HT (30 mg mL^{-1}) and PCBM (24 mg mL^{-1}) and then annealed at 150 °C for 10 min in a glovebox.[9] A mixture of PEDOT:PSS aqueous solution (PH1000) and 2-propanol (volume ratio of 4/1) was coated at the top of the P3HT/PCBM layer, followed by annealing at 150 °C for 10 min. A MWCNT fiber was twisted onto the polymer-coated Ti wire to produce the wire-shaped PSC with lengths of from millimeters

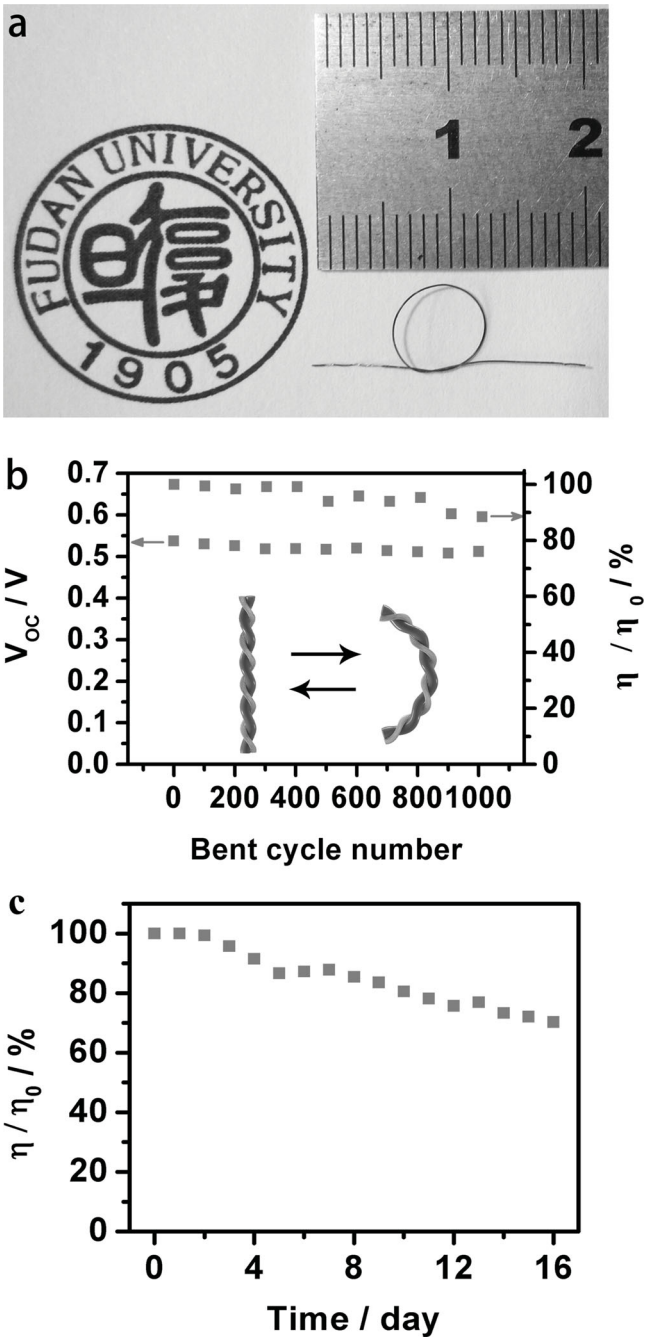

Figure 6. a) Photograph of a knotted wire-shaped PSC. b) Dependence of energy conversion efficiency and voltage on bent cycle number. η_0 and η correspond to the efficiency before and after bending, respectively. c) Dependence of energy conversion efficiency on time for the PSC wire in air. η_0 and η correspond to the as-fabricated device and the one with the time, respectively. The solar cell textile was composed of eight PSC wires.

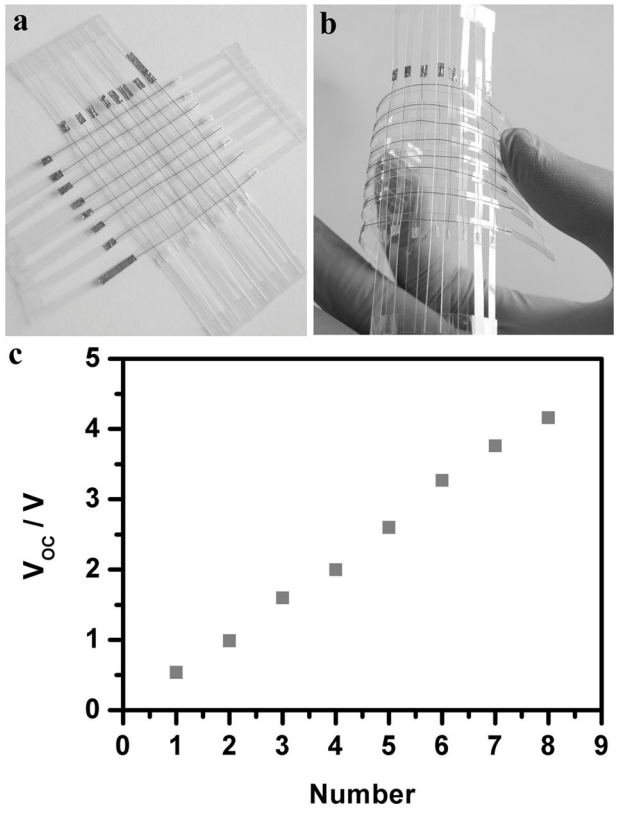

Figure 7. a,b) PSC textile being bent into different structures. c) Dependence of voltage on the number of wire-shaped PSCs that appeared in series in a PSC textile.

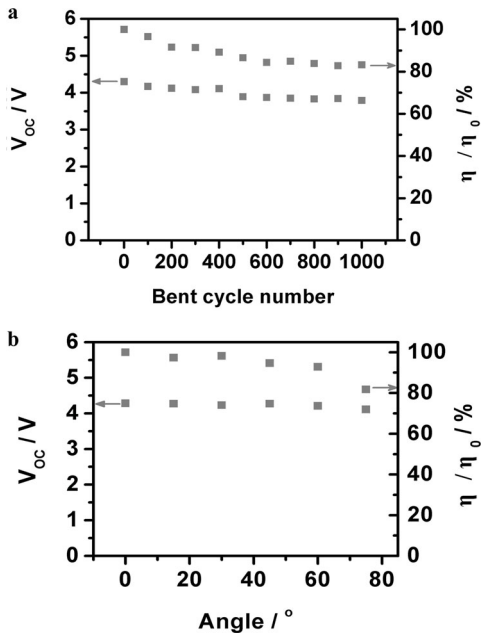

Figure 8. a) Dependence of energy conversion efficiency and voltage on bent cycle number in a solar cell textile. η_0 and η correspond to the efficiencies before and after bending, respectively. b) Dependence of energy conversion efficiency and voltage on the angle between the solar cell textile and substrate with the light source at the top. η_0 and η correspond to the 0 and the other angle, respectively.

to centimeters. For the characterization convenience, the ends of two electrodes were connected to indium by an ultrasonic soldering mate (USM-V, Kuroda Techno). The wire-shaped PSCs could be interlaced and woven into flexible textiles similar to the well-developed textile technology. A Ti wire electrode of a wire-shaped PSC was connected to an MWCNT fiber of a neighboring wire-shaped PSC. In other words, the

wire-shaped PSCs were connected in series to achieve high voltages that depended on the number of wire-shaped PSCs. The remaining Ti wire at one end and MWCNT fiber at the other end were connected to the external facility to record J–V curves of the PSC textile. For the bending measurements, the PSC wires and textiles were folded with bending radii of appropriately 5 mm and 1 cm according to the previous study, respectively.[25]

Supporting Information

Supporting Information is available from the Wiley Online Library or from the author.

Acknowledgements

This work was supported by MOST (2011CB932503, 2011DFA51330), NSFC (91027025, 21225417), STCSM (11520701400, 12nm0503200), Fok Ying Tong Education Foundation, the Program for Professor of Special Appointment at Shanghai Institutions of Higher Learning, and the Program for Outstanding Young Scholars from Organization Department of the CPC Central Committee.

Received: November 14, 2013
Revised: March 4, 2014
Published online:

[1] T. Chen, L. Qiu, Z. Cai, F. Gong, Z. Yang, Z. Wang, H. Peng, *Nano Lett.* **2012**, *12*, 2568.
[2] T. Chen, L. Qiu, Z. Yang, H. Peng, *Chem. Soc. Rev.* **2013**, *42*, 5031.
[3] T. Chen, L. Qiu, H. G. Kia, Z. Yang, H. Peng, *Adv. Mater.* **2012**, *24*, 4623.
[4] Y. Bai, Y. Cao, J. Zhang, M. Wang, R. Li, P. Wang, S. M. Zakeeruddin, M. Gratzel, *Nat. Mater.* **2008**, *7*, 626.
[5] Z. Yang, T. Chen, R. He, G. Guan, H. Li, L. Qiu, H. Peng, *Adv. Mater.* **2011**, *23*, 5436.
[6] G. K. Mor, K. Shankar, M. Paulose, O. K. Varghese, C. A. Grimes, *Nano Lett.* **2006**, *6*, 215.
[7] X. Wang, L. Zhi, K. Mullen, *Nano Lett.* **2008**, *8*, 323.
[8] J. Liu, M. A. G. Namboothiry, D. L. Carroll, *Appl. Phys. Lett.* **2007**, *90*, 133515.
[9] D. Liu, M. Zhao, Y. Li, Z. Bian, L. Zhang, Y. Shang, X. Xia, S. Zhang, D. Yun, Z. Liu, A. Cao, C. Huang, *ACS Nano* **2012**, *6*, 11027.
[10] M. R. Lee, R. D. Eckert, K. Forberich, G. Dennler, C. J. Brabec, R. A. Gaudiana, *Science* **2009**, *324*, 232.
[11] T. Chen, L. Qiu, H. Li, H. Peng, *J. Mater. Chem.* **2012**, *22*, 23655.
[12] J.-H. Park, J.-Y. Kim, J.-H. Kim, C.-J. Choi, H. Kim, Y.-E. Sung, K.-S. Ahn, *J. Power Sources* **2011**, *196*, 8904.
[13] Z. Zhang, X. Chen, P. Chen, G. Guan, L. Qiu, H. Lin, Z. Yang, W. Bai, Y. Luo, H. Peng, *Adv. Mater.* **2014**, *26*, 466.
[14] B. Vigolo, A. Penicaud, C. Coulon, C. Sauder, R. Pailler, C. Journet, P. Bernier, P. Poulin, *Science* **2000**, *290*, 1331.
[15] M. Ye, X. Xin, C. Lin, Z. Lin, *Nano Lett.* **2011**, *11*, 3214.
[16] G. K. Mor, K. Shankar, M. Paulose, O. K. Varghese, C. A. Grimes, *Nano Lett.* **2006**, *6*, 215.
[17] J. Akilavasan, K. Wijeratne, H. Moutinho, M. Al-Jassim, A. R. M. Alamoud, R. M. G. Rajapaksed, J. Bandara, *J. Mater. Chem. A* **2013**, *1*, 5377.
[18] C. Dong, X. Li, X. Fan, J. Qi, *Adv. Energy Mater.* **2012**, *2*, 639.
[19] K. Lim, S. Jung, J.-K. Kim, J.-W. Kang, J.-H. Kim, S.-H. Choa, D.-G. Kim, *Sol. Energy Mater. Sol. Cells* **2013**, *115*, 71.
[20] R. F. Service, *Science* **2003**, *301*, 909.
[21] X. Sun, Z. Zhang, X. Lu, G. Guan, H. Li, H. Peng, *Angew. Chem. Int. Ed.* **2013**, *52*, 7776.
[22] W. Guo, C. Liu, F. Zhao, X. Sun, Z. Yang, T. Chen, X. Chen, L. Qiu, X. Hu, H. Peng, *Adv. Mater.* **2012**, *24*, 5379.
[23] H. Peng, X. Sun, F. Cai, X. Chen, Y. Zhu, G. Liao, D. Chen, Q. Li, Y. Lu, Y. Zhu, Q. Jia, *Nat. Nanotechnol.* **2009**, *4*, 738.
[24] O. K. Varghese, M. Paulose, C. A. Grimes, *Nat. Nanotechnol.* **2009**, *4*, 592.
[25] S. Huang, Z. Yang, L. Zhang, R. He, T. Chen, Z. Cai, Y. Luo, H. Lin, H. Cao, X. Zhu, H. Peng, *J. Mater. Chem.* **2012**, *22*, 16833.